

Supporting Information for

Turbulence-assisted shear exfoliation of graphene using household detergent and a kitchen blender

Eswaraiah Varrla^{1,3}, Keith R Paton^{1,2} Andrew Harvey^{1,3}, Ronan J Smith,^{1,3} Joe McCauley^{1,3} and Jonathan N Coleman^{1,3*}

¹Centre for Research on Adaptive Nanostructures and Nanodevices (CRANN), Trinity College Dublin, Dublin 2, Ireland.

²Thomas Swan & Co. Ltd., Rotary Way, Consett, County Durham, DH8 7ND, United Kingdom.

³School of Physics, Trinity College Dublin, Dublin 2, Ireland.

Residual surfactant content

A known volume of a graphene-FL dispersion was filtered under high vacuum onto an alumina membrane (20 nm pore size and 25 mm diameter). The resulting compact but relatively thick film was washed with ~1L of water and dried overnight in a vacuum oven at temperature of 50° C. The mass of material in the filtered volume of stock dispersion was then determined using a microbalance (~1.2 mg). From thermogravimetric (TGA) analysis (figure S1) of the dried film, we found that 70% of the film was graphitic; the remainder was attributed to residual surfactant. It is to be noted that, the surfactant that we used in this study was washing up liquid (Fairy Liquid) and it has many other ingredients (5-15% anionic surfactant, less than 5% non-ionic surfactant) such as dimethylol-glycol, Benzisothiazolinone, Laurylamine, Dipropylenediamine and perfume etc. This remaining graphitic percentage matches with our earlier result published elsewhere.¹ We are not surprised to find so much residual surfactant in these films due to the commercial wash up liquid. Their considerable thickness makes it very difficult to wash away the surfactant during film formation. Also other losses 5-15 % after 400 C can be attributed to the volatile compounds present in the fairy liquid.

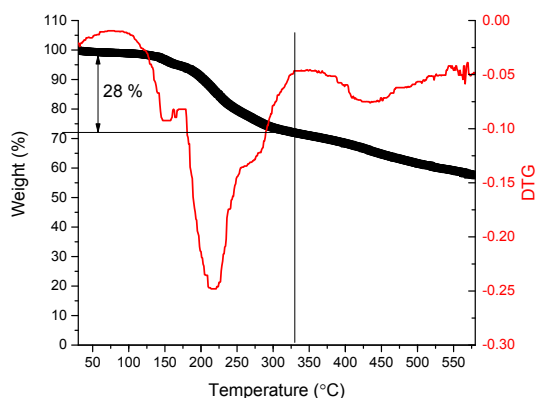


Figure S1: Thermogravimetric analysis of graphene film.

Blender Speed control

The blender as supplied has a two setting speed control (speed 1 and speed 2) and this control results in a blade speed of ~ 13800 and ~ 18000 RPM respectively with ± 2000 rpm. Fine speed control is realised by phase control of the AC waveform applied to the motor as shown below.

A phase control module was used which varies the phase angle of each half cycle of the applied waveform between zero and 180 degrees, depending on the setting of a control potentiometer. This results in a continuously variable fraction of the available power being applied to the motor, allowing the speed to be continuously controlled. The blade rotation speed is measured by sensing the motor shaft rotation. Because of the potentially high blade speeds involved, a solution was needed which would not unbalance the motor. Accordingly a self-adhesive strip of aluminium tape was attached to the fan at the base of the motor shaft. As the motor rotates, this is detected by a reflective optical sensor which outputs one pulse per motor revolution. The resultant pulse train can be measured by means of an oscilloscope or frequency counter. The schematic for the open loop speed control system is shown above. We monitored the RPM from oscilloscope by noting down the values periodically that resulted in bit lower values than it should be initially due to generation of foam from surfactant in the mixing process. The speed of the blade does not changes significantly between batch to batch and changes are within standard errors provided by the Kenwood Company and also confirmed from our measurements from oscilloscope. However, this does not affect our concentration results and trends since it appeared to be same for every batch. However, the speed at initial mixing times

reaches its maximum speed because amount of FL required (to maintain ratio of 8:1) is less and hence foam is less. That is the reason we choose 20 mg/ml for N and V dependence study in the main manuscript.

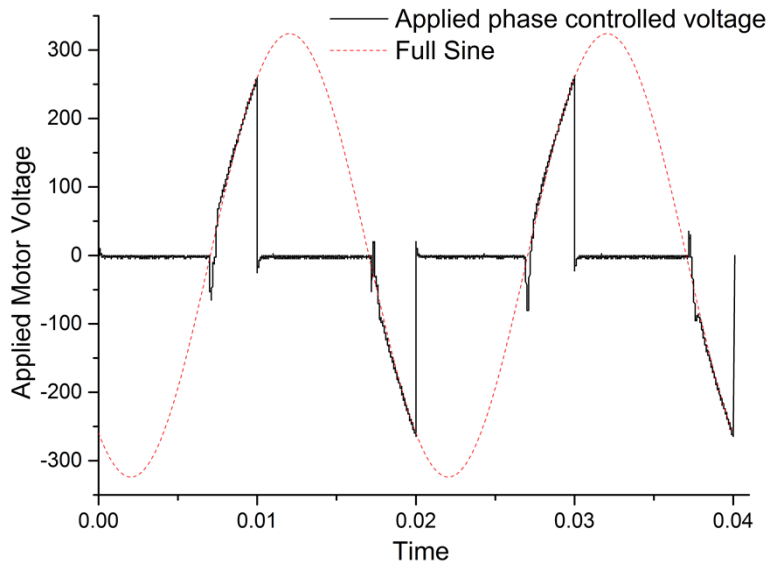


Figure S2: Phase control of the AC waveform.

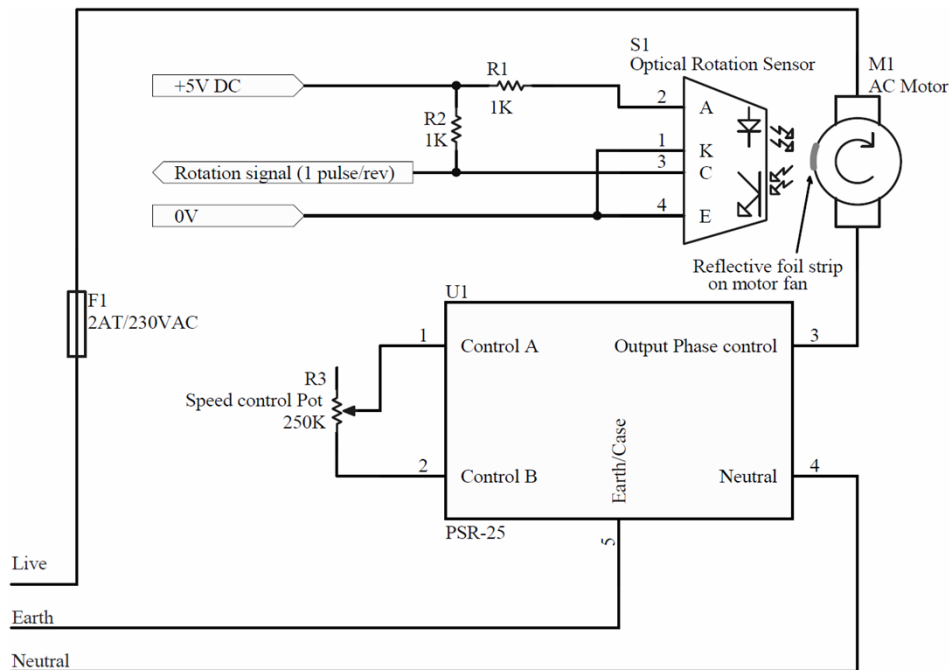
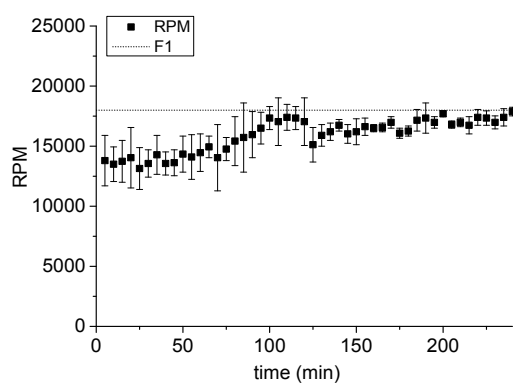


Figure S3: Schematic for the open loop speed control system.



Measurements	RPM	SD
25	3497	180
25	6189	406
25	10657	439
25	14520	486
25	15840	1416
25	18000	2352

Figure S4: RPM of the blade with time showing the stability (left), table explains typical standard deviations involved in measuring RPM from oscilloscope from low to high RPM.

¹ M. Lotya, Y. Hernandez, P. J. King, R. J. Smith, V. Nicolosi, L. S. Karlsson, F. M. Blighe, S. De, Z. M. Wang, I. T. McGovern, G. S. Duesberg, and J. N. Coleman, *Journal of the American Chemical Society*, **131**, 2009, 3611.